Energy Conversion and Management 166 (2018) 402–408

Contents lists available at ScienceDirect

Energy Conversion and Management

journal homepage: www.elsevier.com/locate/enconman

Optimal sizing of a grid-assisted wind-hydrogen system

José G. García Clúa[a,b,*], Ricardo J. Mantz[a,c], Hernán De Battista[a]

[a] Instituto LEICI, UNLP-CONICET, Facultad de Ingeniería, Universidad Nacional de La Plata, C.C.91 (1900) La Plata, Argentina
[b] Departamento de Ingeniería Química, Facultad de Ingeniería, Universidad Nacional de La Plata, Argentina
[c] Comisión de Investigaciones Científicas de la Provincia de Buenos Aires (CICpBA), Argentina

ARTICLE INFO

Keywords:
Hydrogen production
Wind energy
Grid assistance
Electrolyzer sizing

ABSTRACT

Hydrogen obtained from water electrolysis in addition to being sustainable becomes commercially competitive when a high degree of purity is sought. Ideally such purity is achieved by keeping the electrolyzer on a constant and rated power. To satisfy this objective the assistance of the electric grid to deal with the variability of the wind resource was proposed. The disadvantage of this alternative is the failure to ensure a 100% carbon-emission-free hydrogen. The surplus wind energy can be delivered to the grid to optimize the trade-off between purity and cleaning degree. This paper presents a study on how the electrolyzer should be sized – according to the turbine and wind resource – to fully compensate these emissions along the year, that is, to cancel the annual power supplied by the grid.

1. Introduction

When renewable energies are used, the hydrogen obtained from water electrolysis is far more sustainable than the hydrogen obtained from steam methane reforming (SMR) [1]. But that is not better regarding the economic viability, even when energy is extracted from wind – one of the most attractive options [2,3]. However, it does become commercially competitive when a high degree of purity is sought. High-pressure and temperature alkaline electrolyzers generate H_2 with a purity better than 99.97%, which is the quality used in the automotive industry [4]. But this purity is achieved for very strict conditions on the electrolyzer operation; and due to the variability of the wind resource such conditions cannot be guaranteed [5]. Ideally such purity could be achieved by keeping the electrolyzer on a constant and rated power.

The electric grid, if available, can be used to assist the system to satisfy the purity objective. That is, the grid connection will provide electricity in the periods of wind resource shortage. In [6] it is remarked that without extra power from grid the intermittently work of the electrolyzer exerts negative influence on its efficiency, lifetime and hydrogen purity. Even with part time electrolyzer operation to avoid intermittency only limited reductions of the average hydrogen production cost are achieve. Additional advantages of grid assistance were pointed out in previous works. In [7] it is presented as the way the electrolyzer may operate all the time at its design point. As the only down-time would be for maintenance, the system may reach capacity factors of 90%. This would improve the economics by significantly reducing hydrogen cost. In [8] is shown that a combined wind and grid connected hydrogen refuel station can served a higher number of customers. In [9] is ensured that electrolyzer efficiency and hydrogen production is maximized as a consequence of keeping constant the electrolyzer power at its rated value. Another benefit of this operation mode is that the electrolyzer is subjected to less stress [10].

The disadvantage of this alternative is the failure to ensure a 100% carbon-emission-free hydrogen. That is, there is a trade-off between purity degree and cleaning degree. One way to compensate CO_2 emissions is to deliver – if possible – the surplus wind energy to the grid. For this aim, the wind turbine should be oversized as suggested in [11]. The difference is that the wind power excess is not sent to the grid but it is stored in batteries in that work. This have the disadvantage that the greater the power excess, the greater the storage system cost. In [12] is reported the inverse case, where the power delivered to the grid is fixed by the demand and the power excess is sent to the electrolyzer. The absorbed energy determined there, which is a function of the oversize or rather the ratio of the turbine and electrolyzer power, is of particular interest here. In that reference the sizing that optimizes the power excess absorbtion is determined through numerical simulations of the system based on large real wind and demand time series considering different electrolyzer sizes.

There exist other more complex methods of optimum sizing which take into account the stochastic nature of multiple renewable energy sources, electric loads profiles, as well as non-linear responses of the system components, costs and life cycles associated. These can be classified as probabilistic, analytical and iterative methods or a combination of all of them [13–17]. As an example of iterative method it

* Corresponding author at: Instituto LEICI, UNLP-CONICET, Facultad de Ingeniería, Universidad Nacional de La Plata, C.C.91 (1900) La Plata, Argentina.
E-mail address: jose.garciaclua@ing.unlp.edu.ar (J.G. García Clúa).

https://doi.org/10.1016/j.enconman.2018.04.047
Received 12 January 2018; Received in revised form 11 April 2018; Accepted 12 April 2018

can be cited the population-based optimization algorithm proposed in [18] to minimize the energy transfer loss and the levelized cost of hydrogen production.

In the present work, a sizing methodology oriented to a grid assisted wind-hydrogen system is provided to the scientific community. The assistance of the grid is controlled to guarantee the rated operation of the electrolyzer independently of the variations of the wind resource. As a consequence the purity and production rate of the hydrogen is maximized. The grid, in turn, can receive excess power from the wind-hydrogen system. The purpose of the sizing procedure is therefore to find an optimum ratio between wind turbine and electrolyzer rated powers, such that the power supplied by the electric grid is balanced with that received from the surplus of the renewable resource along the year. In this way, the carbon emissions associated with the grid would be compensated and then a more sustainable hydrogen could be produced. A simple probabilistic method based on stochastic parameters of the resource at the turbine location is proposed. The results will be compared with that obtained from a proposed iterative method. The disadvantage of this one is the higher degree of difficulty for implementation.

The paper is structured as follows: Section 2 provides a model description of components of the wind-hydrogen system to be sized; Section 3 presents a sizing methodology based on specifications of the wind turbine and stochastic characteristics of the installation site; Section 4 shows numerical results of the sizing methodology based on simulations in order to verify the theoretical results. Finally, Section 5 summarizes the conclusions.

2. System description

The autonomous system under study consists of a three-bladed horizontal axis turbine directly coupled to a permanent magnet synchronous generator which feeds an alkaline electrolyzer for the hydrogen production. Such devices are coupled to a common DC-bus using suitable power converters. Grid assistance can be incorporated into the same bus as shown in the block diagram of Fig. 1.

2.1. Turbine power converter

The mechanical power captured by the wind turbine for a given wind speed v is [19]:

$$P_T = \frac{1}{2}\rho A_T C_P v^3, \tag{1}$$

where ρ is the air density, A_T is the area swept by the blades and C_P is the power coefficient, which can be modeled by the following empiric formula [20]:

$$C_P = c_1\left(\frac{c_2}{\lambda_i} - c_3\beta - c_4\right)\exp\left(-\frac{c_5}{\lambda_i}\right) + c_6\lambda, \tag{2}$$

$$\frac{1}{\lambda_i} = \frac{1}{\lambda + 0.08\beta} - \frac{0.035}{\beta^3 + 1} \tag{3}$$

The tip-speed-ratio λ is defined as the ratio between de linear speed of the blade tip with respect to the wind speed v,β is the blade pitch angle and the coefficients c_i are $c_1 = 0.5176$, $c_2 = 116$, $c_3 = 0.4$, $c_4 = 5$, $c_5 = 21$, $c_6 = 0.0068$. The dependence of C_P on λ and β is shown in Fig. 2. Note the maximum of the surface at $\lambda = 8.1$ and $\beta = 0$, corresponding to the maximum power coefficient $C_{P,max} = 0.48$. As it was expected, it is less than established by Betz [21]. By substituting $C_{P,max}$ in Eq. (1), the maximum wind power specified by the manufacturer is obtained. The AC-DC converter depicted in Fig. 1 – which couples the wind turbine synchronous generator to the DC-bus – can be used to keep the tip-speed-ratio fixed at λ_0 and ensure the maximum power point. Then the dependence of P_T with v follows a cubic law as it is shown in Fig. 3. The cubic function is valid between the cut-in (v_{min}) and rated wind speed (v_N). From v_N to the cut-out wind speed v_{max} the power must be kept constant at the rated value P_T^N of design. This can be ensure by rotating the blades to increase the pitch angle β [19].

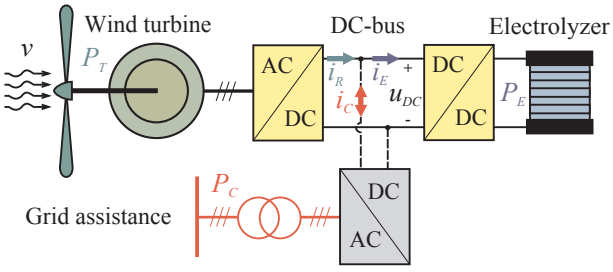

Fig. 1. Scheme of the wind-hydrogen system with assistance of the electric grid.

In this work control strategies applied to the power converter and the pitch actuator are assumed to follow exactly the power curve depicted in Fig. 3. For instance, the minimum projection algorithm proposed for the converter switching in [22] and the proportional controller designed for the pitch servo in [23] can be implemented in order to guarantee the tracking of such reference. For the purpose of the analysis, the electrical, magnetic and mechanical losses of the turbine-generator-converter assembly are neglected and P_T is considered the power delivered to the bus.

2.2. Electrolyzer power converter

The hydrogen production can be characterized by the electrical behavior of the alkaline electrolyzer generating it. The voltage u_E in terminals and the current i_E supplied to such device can be linked by the following empirically expression:

$$u_E(i_E,T_E) = N_S\left[U_{rev} + s\ln\left(\frac{1}{t}i_E + 1\right) + v\ln\left(\frac{1}{w}i_E + 1\right) + \frac{r}{A_E}i_E\right], \tag{4}$$

where N_S is the number of series-connected cells of the electrolyzer stack, A_E is the cell surfacer, U_{rev} is the cell reversible potential and $\{s,t,v,w\}$ models the dependency on the electrolyte temperature T_E of the activation and ohmic irreversibilities or overvoltages as shown in [24].

Since each molecule of hydrogen generated needs two-electron transfer, the hydrogen production rate $\dot{n}_{H_2}$ is proportional to the supplied current i_E, as can be seen in the following expression:

$$\dot{n}_{H_2} = N_S\eta_F 2Fi_E, \tag{5}$$

where F is the Faraday constant and η_F is the Faraday efficiency which increases with i_E according to the formula given in [25]. Furthermore, the electrolyzer current directly affects the quality or purity level Q_{H_2} of the produced hydrogen. This is defined as the ratio between the product gas H_2 and the total volume of the mixture of gases H_2 and O_2. The expression (6) reveals the increase of Q_{H_2} with i_E:

$$Q_{H_2} = 1 - \frac{\dot{n}_{O_2/H_2}}{\dot{n}_{H_2} + \dot{n}_{O_2/H_2}} = 1 - \frac{a_T a_P}{i_E}, \tag{6}$$

where a_T and a_P models the dependency on temperature T_E and pressure P_E respectively as shown in [26].

From the Eqs. (5) and (6) it is inferred that the optimum quantity and quality of the produced H_2 is obtained with the maximum current I_E^N admissible by the electrolyzer. Such rated current can be an assumption or a result of a technical-economic optimization. For instance, high cell areas of the electrolyzer give lower values of I_E^N for the same water utilization factor but with higher investment costs. Here I_E^N is assumed as the maximum current that should be consumed by the electrolyzer to convert all make-up water into hydrogen and oxygen [27].

Consequently, the control objective of the DC-DC converter coupling the electrolyzer to the DC-bus in Fig. 1 is to maintain the current i_E

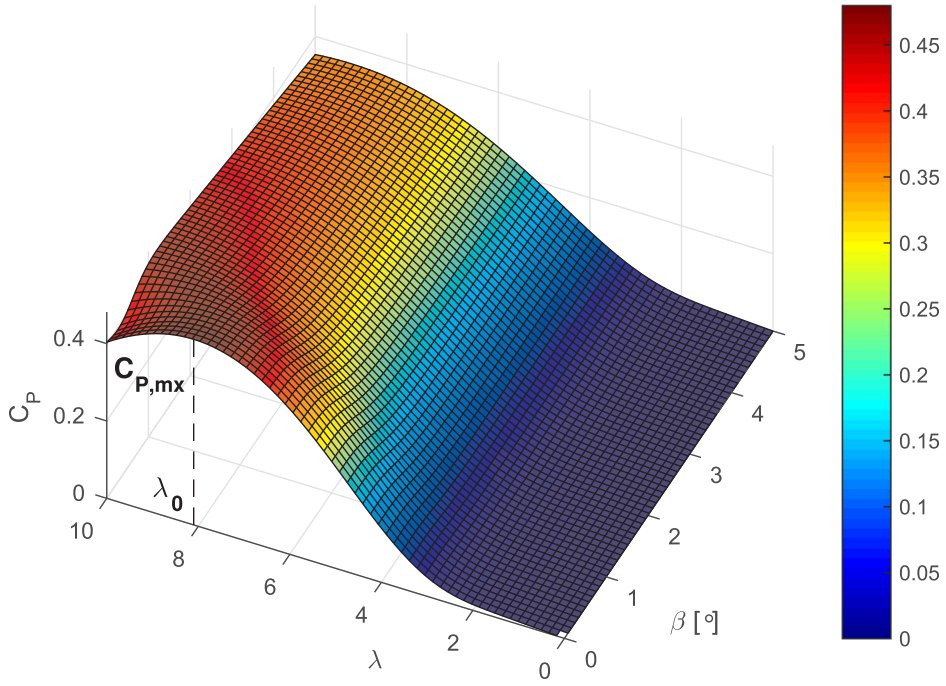

Fig. 2. Power coefficient as a function of the tip-speed-ratio and pith angle.

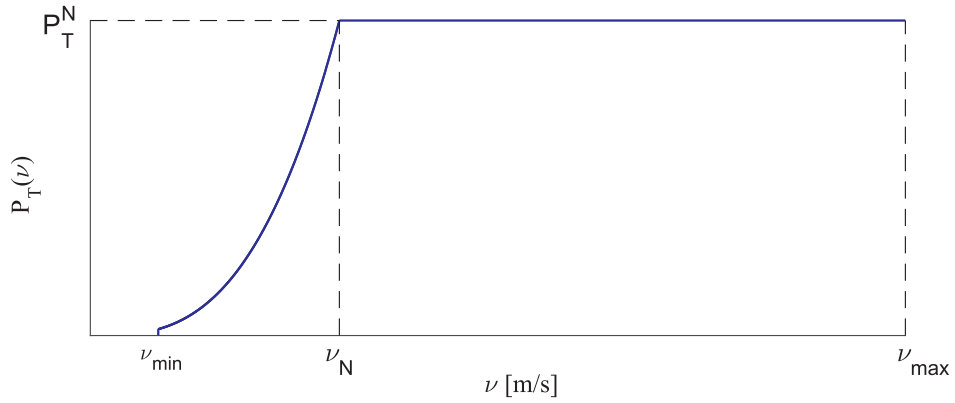

Fig. 3. Turbine power curve specified by the manufacturer.

at the rated value I_E^N to minimized the production cost and maximized the hydrogen purity. Additionally, this is the best electrolyzer operation to meet specifications of the commercial models, which were designed to be fed by the power grid. The control strategy applied to the converter must guarantee the electrolyzer voltage u_E given by the logarithmic expression (4) at the rated current I_E^N and electrolyte temperature T_E. Assuming that the algorithm proposed in [23] is implemented to ensure such voltage and neglecting converter losses, the power demand required to the bus for the electrolysis can be approximated with the following rated power expression:

$$P_E^N = I_E^N u_E(I_E^N, T_E). \tag{7}$$

2.3. Grid power converter

The AC-DC converter of Fig. 1 adapts and controls the electrical assistance provided by the three-phase grid. Eq. (8) shows the assistance in terms of current injected into the DC-bus in case of imbalance between the current demanded by the electrolyzer and the current delivered by the turbine:

$$i_G = i_E - i_R. \tag{8}$$

To regulate i_G a feedback loop that commands the grid converter switching is applied. Among others, min-projection strategy proposed in [22] can be implemented as the controller. If (8) is scaled by the bus voltage u_{DC} – and losses in both wind generation and grid supply are neglected – it can be obtained:

$$P_G(\nu) = P_E^N - P_T(\nu), \tag{9}$$

which is the assistance required by the electrolyzer operating at rated power (ie maximum hydrogen production) for a given wind speed at the turbine hub.

3. Sizing methodology

The methodology proposed for electrolyzer sizing is based on estimating the energy extracted from the grid taking into account the stochastic nature of the renewable resource. As it considers the effect of uncertainty associated with the wind speed in the system design, it could fall into the category of probabilistic optimum sizing methods mentioned in Section 1. One of the advantages of these methods is that energy reliability for the system can be conducted in a quantitative way. To do this, Weibull cumulative probability function is used [28]:

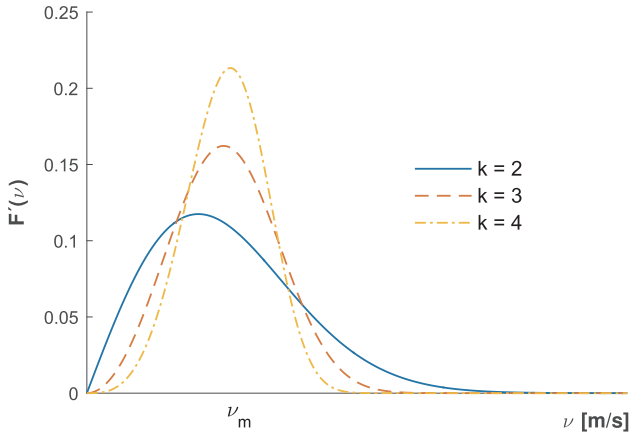

Fig. 4. Weibull probability density.

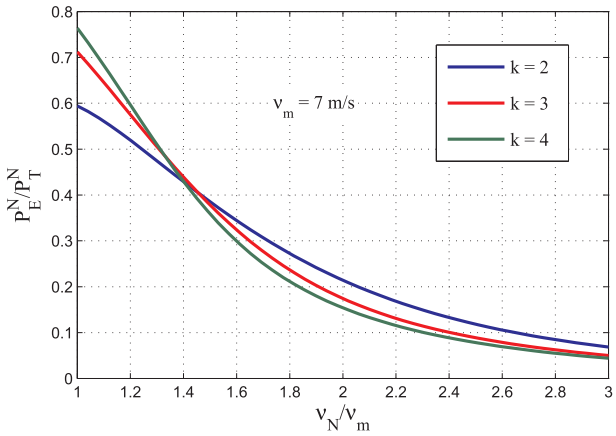

Fig. 5. Electrolyzer rated power that theoretically cancels annual grid power assistance.

$$F(\nu) = 1-\exp(-(\nu/c)^k) \tag{10}$$

where k and c are, respectively, the shape and scale coefficients at a particular site. A more characteristic parameter that emerges from these coefficients is the annual mean wind speed:

$$\nu_m = c\,\Gamma(1 + 1/k), \tag{11}$$

where Γ is the complete gamma function. In Fig. 4 the derivative of F, which is the Weibull probability density, is plotted as a function of the wind speed for a given ν_m and different values of k.

The energy exchanged with the grid can be estimated in the period $T = 1$ year integrating the power (9) weighted by the probability density of each speed ν:

$$E_G = T\int_0^\infty P_G(\nu)F'(\nu)\,d\nu. \tag{12}$$

The aim of the system sizing is to ensure that the net energy exchanged with the grid is minimal throughout the year to compensate CO_2 emissions associated with it. The best scenario would be the one in which the surplus energy sent to the grid in periods of the maximum renewable resource availability equals that supplied by it to the electrolyzer in shortage periods. This ideal case corresponds to a null value – and then minimum – of E_G. By canceling Eq. (12) and replacing P_G with Eq. (9), the following difference of integrals arises:

$$\int_0^\infty P_E^N F'(\nu)\,d\nu - \int_0^\infty P_T(\nu)F'(\nu)\,d\nu \equiv 0 \tag{13}$$

Resolving the second integral in parts according to the wind speed intervals that define the power curve of the turbine – $P_T(\nu)$ in Fig. 3 – the electrolyzer rated power is cleared:

$$P_E^N \underbrace{\int_0^\infty F'(\nu)\,d\nu}_{=1} = \int_{\nu_{\min}}^{\nu_N} \frac{1}{2}\rho A\nu^3 C_{P,max}F'(\nu)\,d\nu + \int_{\nu_N}^{\nu_{\max}} P_T^N F'(\nu)\,d\nu \tag{14}$$

The optimal sizing can be easily characterized in Eq. (14) through the electrolyzer and turbine rated power ratio taking common factor P_T^N and considering that it is the Eq. (1) evaluated in $C_{P,max}$ and ν_N:

$$P_E^N/P_T^N = \int_{\nu_{\min}}^{\nu_N} (\nu/\nu_N)^3 F'(\nu)\,d\nu + F(\nu_{\max}) - F(\nu_N). \tag{15}$$

Since the integral of Eq. (15) cannot be calculated analytically, it is solved numerically and plotted in Fig. 5 as a function of the rated-to-annual mean wind speed ratio for some values of k. It was considered a mean wind speed $\nu_m = 7$ m/s and the ideal power curve $P_T(\nu)$ of a turbine like the one in [29].

Assuming that a commercial turbine of rated power and wind speed is available, Fig. 5 allows the following comments on the electrolyzer and system placement choice:

- In all cases, the sizing objective is fulfilled for electrolyzer rated powers P_E^N lower than the turbine rated power P_T^N. The lower the electrolyzer power P_E^N, the higher the rated speed ν_N of the turbine with respect to the annual mean speed ν_m of the renewable resource at the site. This has the disadvantage of the wastage of the turbine, which would rarely produce the power P_T^N for which it was designed. That is, the capacity factor of the turbine would be very low. It can be seen also that the optimal power P_E^N is not very sensitive to the shape coefficient k of the resource.
- The advantage for electrolyzer powers P_E^N closer to the turbine power P_T^N is the approaching of the annual mean wind speed to the rated of the turbine. The tendency for values $\nu_N < \nu_m$ is not considered because of being an inadequate turbine selection. The advantage near the limit $\nu_N = \nu_m$ is a better turbine utilization (ie, a greater capacity factor) while the disadvantage is a higher sensitivity to the shape coefficient k of the optimum power P_E^N. It depends on the place and the season of the year, among other factors. Values of $k > 2$ correspond to distributions skewed towards higher wind speeds, indicating greater probability of occurrence of them in such places and/or seasons. There are several techniques that adjust the Weibull distribution to the data measured at a certain geographic location in order to properly determine k and ν_m [30].
- Electrolyzer powers P_E^N around 0.43 times the rated turbine P_T^N result in a good trade-off between capacity factor and shape coefficient k dependence. In fact the dependence on k is minimal for that electrolyzer to turbine rated power ratio. On the other hand the corresponding rated to mean wind speed belong to the range generally recommended for the wind turbine location [31].

4. Simulation results

In this section, the optimal electrolyzer size found theoretically in Section 3 for a given commercial turbine and wind resource is corroborated using numerical simulation. The procedure followed responds to the class of iterative sizing methods mentioned in Section 1. Several simulations are carried out taking into account different sizes of the system devices for a certain climate time series of the site. The energy extracted from the grid during the simulation time is calculated for each size and the minimum one determine the optimum size. Note that the use of a certain wind speed time series here makes this method a kind of deterministic approach and therefore less accurate than the probabilistic one proposed.

The overall system is modeled using the Simulink SimPowerSystems toolbox as it is shown in Fig. 6. It can be seen three current dependent sources which represent the main subsystems of the wind–hydrogen connected to the common DC-bus. The I_R current delivered to the bus is the result of controlling the AC-DC converter of the wind turbine to

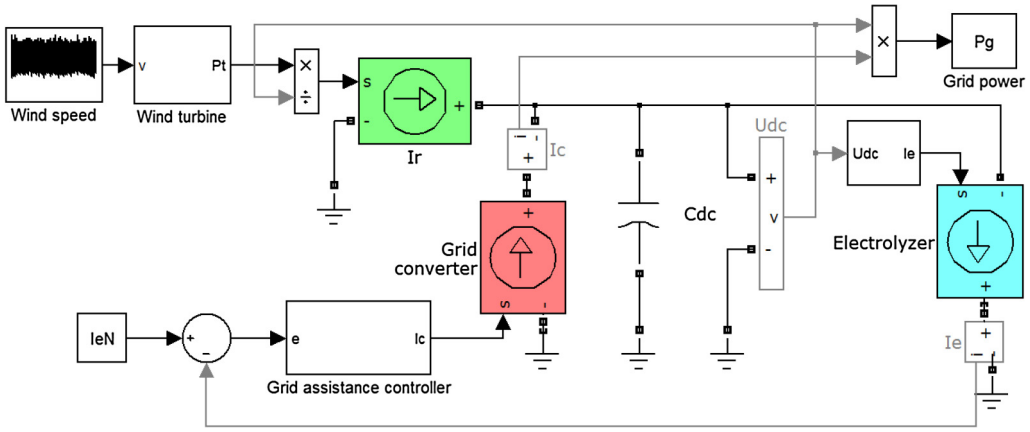

Fig. 6. Model of the grid assistance using the Simulink SimPowerSystems toolbox.

follow the ideal power curve $P_T(\nu)$ depicted in Fig. 3. It is contained in the ν-dependent P_T block. The wind speed source is a interpolated time sequence generated randomly by the Weibull distribution of Eq. (10). The I_E current consumed by the electrolyzer is linked to the bus voltage U_{DC} through a nonlinear block containing the electrical characteristics of the equipment to be evaluated. The electrolyzer converter control is ignored for the sake of simplicity in order to focus in the power of the Eq. (7), which is independent of it neglecting electrical losses. The I_C current supplied by the grid acts as the output of the assistance controller which maintain the electrolyzer power fixed at its rated value I_E^N. The C_{DC} capacitor models the DC-bus response to fast power imbalances. The P_G output label is the measure of the instant grid power to be minimized along a year or the time considered.

In Fig. 7 is explained through a flowchart how are obtained the series of simulations of the built model that allow to reproduce the theoretical curves of optimal electrolyzer size. Broadly speaking, the flowchart consists of two nested "for" loops. The outer loop is entered by setting the shape coefficient k^* and the annual mean wind speed ν_m of the renewable resource. The inner loop is entered by setting a percentage of ν_m higher than 100% as the rated wind speed ν_N of the turbine. This value sets the rated power P_T^N of the turbine given by Eq. (1). At each iteration of this "for" loop, the model is simulated by setting different rated power values P_E^N of the electrolyzer, as percentages of P_T^N always lower than 100%. From each model simulation, the total energy E_G contributed by the grid is extracted. This is calculated integrating the output P_G over the simulation time. Once the entire range of possible values of P_E^N is covered, the inner loop is exited and a curve $f(x)$ is drawn, where at each value $x = P_E^N$ a value $f(x) = E_G$ is assigned. Then the value x^* is determined graphically where the curve cross the x axis, that is, where $f(x^*) = 0$ is satisfied. That will be the optimal electrolyzer rated power for the given ν_m speed and that will enable the start of a new iteration of the outer loop with a different value ν_N. The outer "for" loop is exited once all the iterations needed to cover the desired values range of ν_N have been run. That is when the routine ends.

The results of the simulations carried out according to the flowchart of Fig. 7 for $\nu_m = 7$ m/s and $k = \{2,3,4\}$ are shown in Figs. 8–10. These are wind resource conditions that allow comparison with the theoretical curves estimated in Section 3.

Note that the optimal electrolyzer rated power obtained by simulation for eleven distinct values of rated power and wind speed of the turbine deviates relatively little from the estimated curves for each value of k. In particular, the higher deviation for $k = 2$ observed in Fig. 8 is reduced significantly for ν_N speeds around $1.4\nu_m$, which corresponds to the turbine size recommended for the region with the considered wind availability. For the case of $k = 2$ and $\nu_m = 7$ m/s, the rated speed recommended for the turbine would be $\nu_N = 9.8$ m/s and the rated power, through Eq. (1), $P_T^N = 1.5$ MW. Then, according to the theoretical and numerical results, the optimal electrolyzer rated power would be approximately $P_T^N = 0.65$ MW.

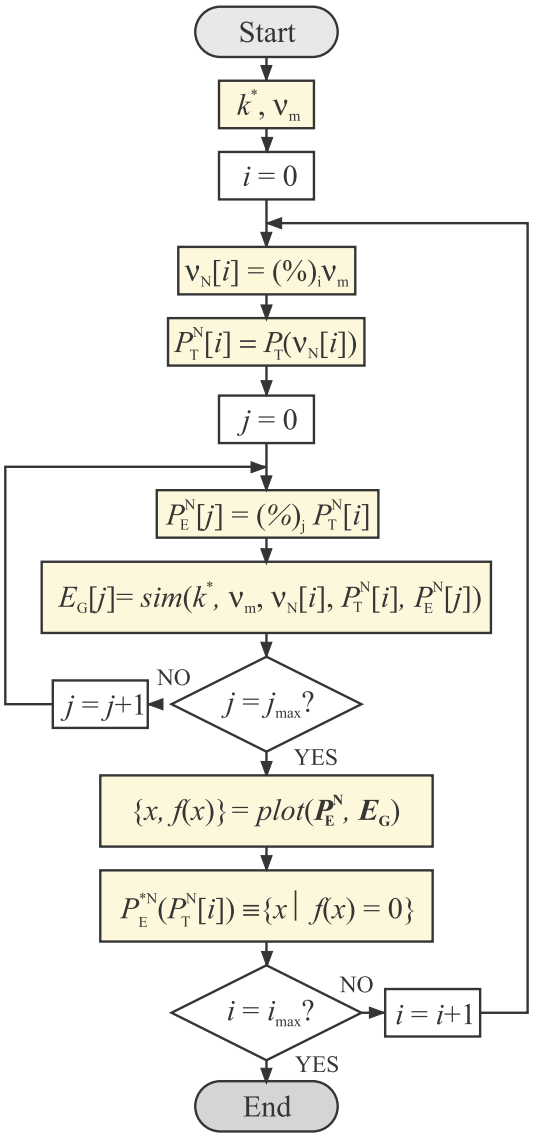

Fig. 7. Flowchart that commands the model simulation.

It should be clarified that to obtain the optimal sizing of the eleven ν_N/ν_m ratios indicated in Figs. 8–10, for three possible values of k, forty

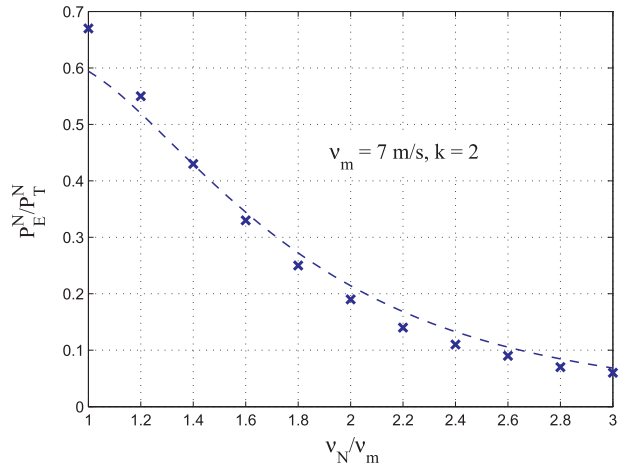

Fig. 8. Simulation (× ×) vs. estimation (- -) results for k = 2.

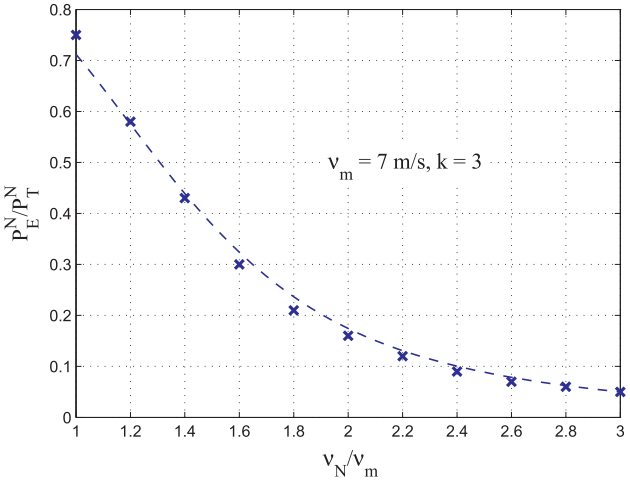

Fig. 9. Simulation (× ×) vs. estimation (- -) results for k = 3.

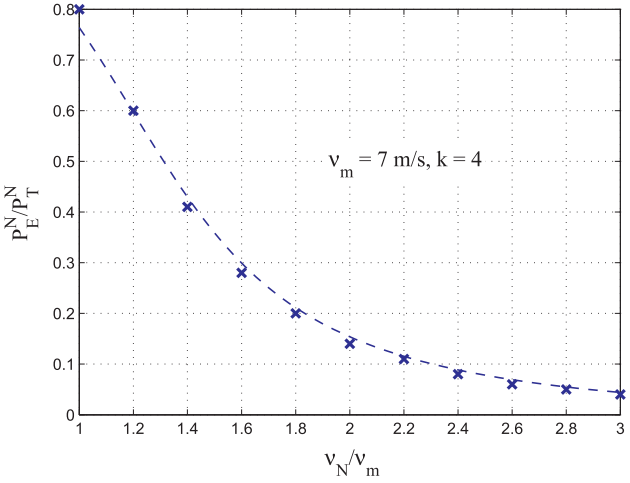

Fig. 10. Simulation (× ×) vs. estimation (- -) results for k = 4.

different P_E^N/P_T^N ratios into the 0–100% range were considered. Taking into account the time step of 1 min used in each simulation the time window was limited to three months, which is equivalent to about 1.10^5 time iterations.

5. Conclusions

The main contribution of this work is to provide an optimum sizing for a grid assisted wind-hydrogen system. Taking into account the Weibull probability density of the wind resource the theoretical method proposed gives the electrolyzer to turbine power ratio such that the system exhibits a virtual autonomous behavior throughout the year. The numerical method show through iterative simulations the same results based on large wind speed time series having the stochastic characteristics of the renewable resource.

The power ratio curves obtained as a function of the annual mean wind speed ν_m for different values of the shape factor k allow to draw some conclusions in connection with the renewable resource. One of them is that although the influence of ν_m predominates in the power ratio, as expected, the influence k also has its importance. This can be observed at the curves in particular for values of ν_m close to the rated wind speed ν_N. The reason for the greater influence of k in such a case is the non-linearity imposed by the rated power saturation at the turbine curve. However it can be noted a special case when the turbine fulfills the ratio $\nu_m/\nu_N = 1.4$ where the optimal sizing becomes independent of the shape factor.

Another conclusion more related to the turbine design is that the range (1.67, 1.77) of the ratio ν_N/ν_m recommended in [31] turns out to be an intermediate point on the trade-off between turbine and resource utilization. That is, for $\nu_N/\nu_m < 1.67$ the electrolyzer uses better available turbine power but wind potential of the site is wasted. On the other hand for $\nu_N/\nu_m > 1.77$ opposite happens.

In case the turbine size is not defined a priori, it should be chosen among the different options meeting the optimum power ratio. That choice should meet other criteria which were not taken into account in this work, such us capital and electricity costs, hydrogen demand, geopolitical location, etc. Each of these criteria introduces new parameters that enrich the optimization method but perhaps making it too complex for the purpose it was originally planned.

Funding

This work was supported by ANPCyT (PICT 2015-3586), CONICET (PIP 112-201501-00837), UNLP (11/I216) and CICpBA of Argentina.

References

[1] Nikolaidis P, Poullikkas A. A comparative overview of hydrogen production processes. Renew Sustain Energy Rev 2017;67:597–611.
[2] Kroniger D, Madlener R. Hydrogen storage for wind parks: a real options evaluation for an optimal investment in more flexibility. Appl Energy 2014;136(Supplement C):931–46.
[3] Mohsin M, Rasheed A, Saidur R. Economic viability and production capacity of wind generated renewable hydrogen. Int J Hydrogen Energy 2018;43(5):2621–30.
[4] Serna Álvaro, Yahyaoui I, Normey-Rico JE, de Prada C, Tadeo F. Predictive control for hydrogen production by electrolysis in an offshore platform using renewable energies. Int J Hydrogen Energy 2017;42(17):12865–76.
[5] Ursúa A, Barrios EL, Pascual J, Martín IS, Sanchis P. Integration of commercial alkaline water electrolysers with renewable energies: limitations and improvements. Int J Hydrogen Energy 2016;41(30):12852–61.
[6] Zhang G, Wan X. A wind-hydrogen energy storage system model for massive wind energy curtailment. Int J Hydrogen Energy 2014;39(3):1243–52.
[7] Sherif S, Barbir F, Veziroglu T. Wind energy and the hydrogen economy -review of the technology. Sol Energy 2005;78:647–60.
[8] Nistor S, Dave S, Fan Z, Sooriyabandara M. Technical and economic analysis of hydrogen refuelling. Appl Energy 2016;167:211–20.
[9] García Clúa J, Mantz R, De Battista H. Evaluation of hydrogen production capabilities of a grid-assisted wind-H2 system. Appl Energy 2011;88(5):1857–63.
[10] Valverde L, Pino F, Guerra J, Rosa F. Definition, analysis and experimental investigation of operation modes in hydrogen-renewable-based power plants incorporating hybrid energy storage. Energy Convers Manage 2016;113:290–311.
[11] Dutton A, Bleijs J, Dienhart H, Falchetta M, Hug W, Prischich D, et al. Experience in the design, sizing, economics, and implementation of autonomous wind-powered hydrogen production systems. Int J Hydrogen Energy 2000;25(8):705–22.
[12] Pino FJ, Valverde L, Rosa F. Influence of wind turbine power curve and electrolyzer operating temperature on hydrogen production in wind-hydrogen systems. J Power Sources 2011;196(9):4418–26.
[13] Luna-Rubio R, Trejo-Perea M, Vargas-Vázquez D, Ríos-Moreno G. Optimal sizing of

renewable hybrids energy systems: a review of methodologies. Sol Energy 2012;86(4):1077–88.
[14] Erdinc O, Uzunoglu M. Optimum design of hybrid renewable energy systems: overview of different approaches. Renew Sustain Energy Rev 2012;16(3):1412–25.
[15] Castañeda M, Cano A, Jurado F, Sánchez H, Fernández LM. Sizing optimization, dynamic modeling and energy management strategies of a stand-alone PV/hydrogen/battery-based hybrid system. Int J Hydrogen Energy 2013;38(10):3830–45.
[16] Feroldi D, Zumoffen D. Sizing methodology for hybrid systems based on multiple renewable power sources integrated to the energy management strategy. Int J Hydrogen Energy 2014;39(16):8609–20.
[17] Khatib T, Ibrahim IA, Mohamed A. A review on sizing methodologies of photovoltaic array and storage battery in a standalone photovoltaic system. Energy Convers Manage 2016;120:430–48.
[18] Sayedin F, Maroufmashat A, Sattari S, Elkamel A, Fowler M. Optimization of Photovoltaic Electrolyzer Hybrid systems; taking into account the effect of climate conditions. Energy Convers Manage 2016;118:438–49.
[19] Bianchi F, De Battista H, Mantz R. Wind turbine control systems. Springer; 2007.
[20] Xia Y, Ahmed KH, Williams BW. Wind turbine power coefficient analysis of a new maximum power point tracking technique. IEEE Trans Industr Electron 2013;60(3):1122–32.
[21] Manwell J, McGowan J, Rogers A. Wind energy explained: theory, design and application, 2nd ed.; 2010.
[22] García Clúa JG, Mantz RJ, De Battista H, Gallegos NG. Stabilisation of grid assistance for a renewable hydrogen generation system by min-projection strategy. IET Control Theory Appl 2016;10(2):183–9.
[23] García Clúa J, De Battista H, Mantz R. Control of a grid-assisted wind-powered hydrogen production system. Int J Hydrogen Energy 2010;35(11):5786–92.
[24] Ursúa A, Sanchis P. Static dynamic modelling of the electrical behaviour of a commercial advanced alkaline water electrolyser. Int J Hydrogen Energy 2012;37(24):18598–614. 2011 International Workshop on Molten Carbonates & Related Topic.
[25] Ulleberg Ø. Modeling of advanced alkaline electrolyzers: a system simulation approach. Int J Hydrogen Energy 2003;28(1):21–33.
[26] Kirati S, Hammoudi M, Mousli I. Hybrid energy system for hydrogen production in the Adrar region (Algeria): production rate and purity level. Int J Hydrogen Energy 2018;43(6):3378–93.
[27] Milewski J, Guandalini G, Campanari S. Modeling an alkaline electrolysis cell through reduced-order and loss-estimate approaches. J Power Sources 2014;269:203–11.
[28] Wind turbines – part 1: design requirements. IEC 61400-1. International Electrotechnical Commission, 3rd ed.; 2005.
[29] Gasch R, Twele J, editors. Wind power plants. Fundamentals, design, construction and operation. 2nd ed.Berlin: Springer-Verlag; 2012.
[30] Khahro SF, Tabbassum K, Soomro AM, Dong L, Liao X, et al. Evaluation of wind power production prospective and Weibull parameter estimation methods for Babaurband, Sindh Pakistan. Energy Convers Manage 2014;78(Supplement C):956–67.
[31] Burton T, Jenkins N, Sharpe D, Bossanyi E. Wind energy handbook. 2nd ed. Wiley; 2011.